Communications to the Editor

Local Dynamics of Polyisobutylene Revisited

K. Karatasos* and J.-P. Ryckaert

Department of Physics, Polymer Physics CP-223, Université Libre de Bruxelles, Bd. du Triomphe, 1050 Brussels, Belgium

Received May 21, 2001

Revised Manuscript Received July 12, 2001

Although PIB is sterically strained by the existence of the methyl groups, it exhibits a surprisingly low glass transition temperature ($T_g \simeq 200$ K) and an unusually low specific volume compared to those of its vinyl counterpart. It must be noted that a similar "T_g anomaly" is observed between other pairs of vinylidene−vinyl polymers, like poly(vinyl chloride) (PVC) and poly(vinylidene chloride) and poly(vinyl fluoride) (PVF) and poly(vinylidene fluoride).[1] Previous computational and simulational efforts contributed to the elucidation of the conformational characteristics[2−5] of PIB, to which its high packing efficiency (and thus its low permeability) should ultimately be related.[6,7] Our results on PIB melts in the 300−600 K temperature regime confirm the existence[5] and lead to the characterization of an additional skeletal relaxation process related to cooperative jumps of small amplitude which originate from the doubling of the main peaks in the dihedral angle distribution function.[4] This process occurs on a time scale of 10−40 ps depending upon temperature. It exhibits a much weaker temperature dependence compared to the usual segmental relaxation process which is mainly driven by gauche−trans skeletal jumps. The latter occurs on a slower time scale but remains accessible within our nanosecond long runs. The presence of the new process justifies a reinterpretation of experimental results on the segmental relaxation.

Segmental dynamics of PIB has been the object of some puzzling observations. While in dielectric relaxation spectroscopy (DRS) and for neutron spin echo (NSE) data[8,9] the segmental process was found to follow the temperature dependence of the rheologically determined[10] shift factors (in agreement with the observed thermorheological simplicity of PIB[11]), nuclear magnetic resonance (NMR)[12−14] and electron spin resonance (ESR)[15] measurements yielded a significantly weaker temperature dependence. As noticed in ref 13, the case of PIB constitutes in this respect a prominent exception, since earlier NMR measurements in several other polymers were consistent with the rheological behavior. The present molecular dynamics (MD) study is focused on the skeletal dynamics of PIB, more particularly upon the interpretation of correlation functions which allow these motions to be probed experimentally. It is within the targets of this work to show how the various experimental observations can be reconciled in a unique framework.

PIB dynamics was explored in a system comprised by five chains of 25 monomers each, brought to bulk density under constant pressure and temperature conditions (NPT ensemble). An equilibration period of 0.5−2 ns depending on the temperature was performed prior to constant energy and volume (NVE) production runs. Following this procedure, trajectories at temperatures $T = 300$, 345, 388, 446, 496, and 603 K (a range where the α and β processes are essentially merged[8]) were generated, using a time step of 1 fs with configurations saved every 0.5 ps. The simulations were performed with the DL_POLY molecular dynamics package.[16] Details on the generation of the starting configurations and the force field parametrization, together with certain static/conformational and dynamic properties of the model, are described elsewhere.[17] For comparison to ^{13}C NMR experiments, the second-order autocorrelation function (ACF)

$$G(t) = \frac{1}{2}\langle 3\cos^2\theta(t) - 1\rangle \tag{1}$$

was calculated. Here $\theta(t)$ describes the orientation of a skeletal C−H bond vector while the averaging was performed over all the equivalent C−H bonds and all the time origins. Space resolution over the backbone hydrogens' motion was obtained by means of the incoherent dynamic structure factor

$$S(q,t) = \left\langle \sum_{i=1}^{N} \frac{\sin(q\Delta r_i(t))}{q\Delta r_i(t)} \right\rangle \tag{2}$$

where q is the magnitude of the scattering vector and $\Delta r_i(t) = ||\vec{r}_i(0) - \vec{r}_i(t)||$ is the magnitude of the displacement of a hydrogen atom. Conformational changes were accounted for by monitoring the transition rates between the equilibrium states.

Conventionally, a number of different models may be invoked for the analysis of time domain neutron scattering[8,18] and NMR[14] data. Nevertheless, to analyze the $G(t)$ and $S(q,t)$ spectra in a unified model-independent fashion, we calculated the corresponding distribution of relaxation times (DRT).[19] In this approach dynamic correlation/scattering functions were described as a continuous distribution of exponential decays according to

$$C(t) = \int_{-\infty}^{+\infty} F(\ln(\tau))\mathrm{e}^{-t/\tau}\mathrm{d}\ln\tau \tag{3}$$

where $F(\ln(\tau))$ symbolizes the normalized distribution function. In a DRT spectra distinct motional processes appear as separate peaks. A characteristic time (CT) for a process appearing in the spectra can be calculated as $\tau = \int_{\Delta\tau_i}\tau F(\ln(\tau))\mathrm{d}\ln\tau / \int_{\Delta\tau_i} F(\ln(\tau))\mathrm{d}\ln\tau$, where $\Delta\tau_i$ indicates the time interval over which this process extends. An

* To whom correspondence should be addressed.

10.1021/ma010869h CCC: $20.00
Published on Web 09/12/2001

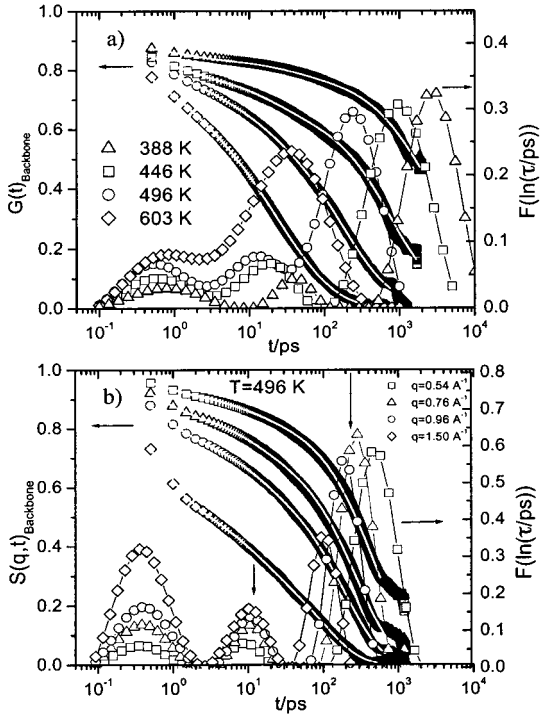

Figure 1. (a) Left axis: autocorrelation functions $G(t)$ at the four higher temperatures for the reorientation of the backbone C−H bonds. The lines through the points show the result of the fit from eq 3. Right axis: corresponding DRTs. (b) Left axis: incoherent dynamic structure factor at $T = 496$ K describing backbone hydrogens' motions for scattering vectors $q = 0.54$ Å^{-1}(□), $q = 0.76$ Å^{-1} (△), $q = 0.95$ Å^{-1} (○), and $q = 1.50$ Å^{-1} (◇). The lines through the points show the result of the fit from eq 3. Right axis: the respective DRTs. The vertical arrows indicate the location of the CTs of the respective $G(t)$ DRT peaks at $T = 496$ K (○ in panel a).

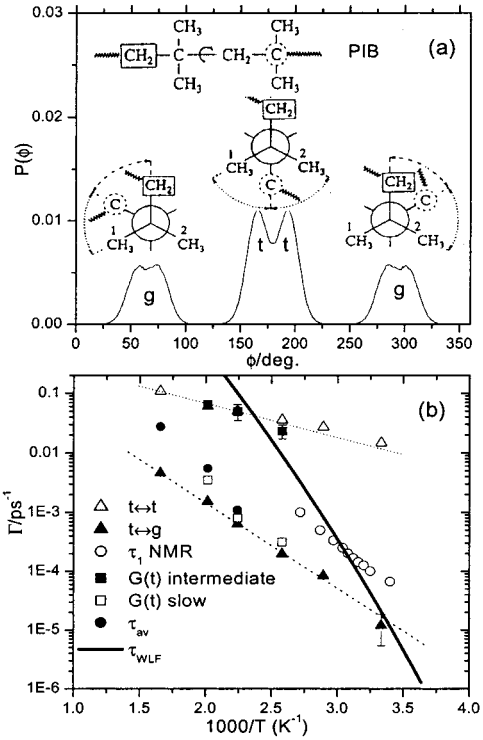

Figure 2. (a) Distribution (symmetrized) of backbone torsional angles at $T = 388$ K showing the gauche (g) states and the double trans (t) maxima, together with schematical representations of the conformational states. (b) Transition rates vs $1/T$ for (t ↔ g) (▲) and (t ↔ t) (△) jumps. Dotted lines are guides for the eye. Inverse characteristic times for the slower (□) and the intermediate (■) processes appearing in the DRTs of Figure 1a; (●) τ_{av} of $G(t)$; (○) τ_1 NMR relaxation times for reorientation of backbone C−H bonds.[13] Error bars are shown if they are larger than the symbol size. Thick solid line denotes the experimental Williams−Landel−Ferry (WLF) behavior.

overall average time τ_{av} is calculated if the integration is performed over the entire time window.

Figure 1 shows $G(t)$ and $S(q,t)$ curves for different temperatures and scattering vectors, respectively, together with the corresponding DRT spectra. Focusing on the $G(t)$ behavior, the relaxation process at the time scale of 1 ps can be assigned to fast librational motions around the torsional energy minima.[20] At longer time scales and in the examined temperature range, instead of the expected single segmental process, two individual processes are resolved at temperatures below $T = 603$ K. The CT of the slower process (as indicated by the location of its maximum) exhibits a stronger temperature dependence. Because of this fact, the two modes merge at a higher temperature, resulting in a single broad peak ($t \simeq 40$ ps) at $T = 603$ K. The behavior of the dynamic structure factor at constant temperature ($T = 496$ K) and at four scattering vectors is shown in Figure 1b. The same processes appear in the $S(q,t)$ dynamics as well. As discussed in ref 17, at the same temperature the $G(t)$ dynamics are approximately reproduced by $S(q,t)$ behavior at a scattering vector close to the first peak of the static structure factor[21] $q = 0.95$ Å^{-1}. This occurrence is marked in Figure 1b by the vertical arrows which indicate the peak positions observed at the same temperature in $G(t)$ (Figure 1a). The fact that the slower relaxation is q-dependent alludes to segmental motion behavior, while the apparent q-independent dynamics of the intermediate mode in this q range implies a constricted motion[22] with a very short characteristic length scale.

A way to arrive at a more conclusive identification of the elementary mechanisms underlying this dynamic picture is provided by examining the conformational changes associated with backbone motion. In Figure 2b, the transition rates between the equilibrium conformational states (as defined by the peaks of the torsional angle probability distribution $P(\phi)$, Figure 2a) are compared to the rates (inverse CTs) of the intermediate and the slower peaks appearing in the DRTs of the $G(t)$ autocorrelation functions. The types of conformational transitions through which backbone motion is realized in PIB are those between the trans-to-gauche (t−g) and the trans-to-trans (t−t) states. It must be stressed here that the splitting of the trans maxima in two equivalent states is a specific feature of PIB, not observed in its vinyl analogue. The close agreement between the inverse CTs and the transition rates leads to an unambiguous identification of the relaxation processes described in Figure 1: the intermediate mode is associated with the t−t conformational jumps while the slow process (at this temperature range) is a manifestation of the t−g transitions.

In Figure 2b the τ_{av} value for the $G(t)$ function is also shown for the three higher temperatures where the decorrelation is almost complete within the simulation time window. As the temperature decreases, τ_{av} becomes more and more heavily weighted by the slow process.

NMR spin−lattice ^{13}C relaxation measurements in the temperature range 270−400 K dedicated to the

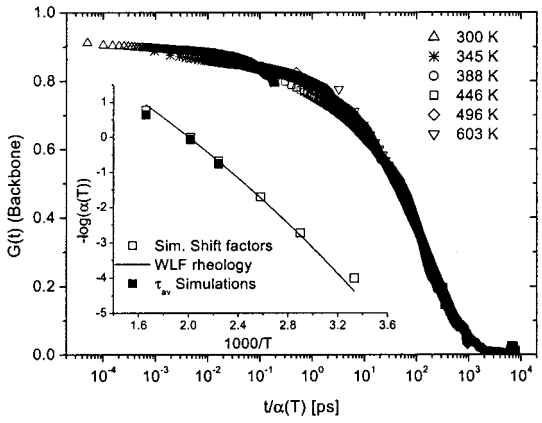

Figure 3. $G(t)$ spectra shifted in order to superpose. Inset: comparison of the shift factors: obtained by shifting the $G(t)$ autocorrelation functions (□), from rheology (solid line), and from the average times τ_{av} calculated by the simulations (■), at the three higher temperatures.

study of the skeletal C−H vector reorientational dynamics of PIB have been interpreted either in terms of the DLM model[13] or in terms of other motional models consisting of a rapid decay of $G(t)$ followed by a slower main relaxation (e.g., stretched exponential).[14] This results for PIB into a virtually model-independent main relaxation time τ_1 which is reported in Figure 2b. In the same figure, we indicate the WLF function describing the segmental dynamics relaxation times obtained from rheology and dielectric data.[8] As mentioned earlier, τ_1 shows a weaker temperature dependence than the one predicted by WLF.[13] Comparing simulation to experimental data, it is interesting to notice that, apart from a vertical shift in the y-axis (accounting for a factor by which simulation times appear to be slower[17]), the temperature dependence of the NMR relaxation time τ_1 is essentially parallel to that of the inverse t−g transitions rates observed in the simulations, while the temperature dependence of the experimentally determined WLF is better described by the τ_{av} behavior of $G(t)$. The question regarding the mismatch between the behavior of the τ_1 relaxation times obtained by certain spectroscopic techniques and the temperature dependence which describes consistently rheological, DRS, and NSE behavior (segmental process) can now be addressed in light of our simulation results.

To appreciate the NMR data, it is important to recall that NMR probes the Fourier transform of $G(t)$ at frequencies which are typically in the 100−500 MHz range. In PIB, simulations reveal an intermediate process in the 10−40 ps regime, depending upon temperature. Given the probed frequencies and the type of motional models used in NMR data interpretation, the process associated with the t−t transitions will be merged with the usual "fast" librational process which takes place on the picosecond time scale and which is usually treated as a temperature-independent contribution. Consequently, the slow process dominated by t−g jumps will furnish the "NMR" main relaxation time.

In the rheological and the NSE measurements, the analysis of the temperature dependence of the relevant correlation function is based on an optimal time−temperature superposition (TTS) over a time span including all elementary processes. For rheological measurements above 300 K, the WLF function is based on the temperature evolution of the (zero frequency) shear viscosity while in the NSE experiments,[8] the intermediate coherent scattering function is probed in a time window starting at a few picoseconds and covering 3 decades in time. In the latter case, TTS with the rheological shift factors was observed at fixed q over the whole range of diffusion vectors explored. The outcome from the application of the TTS principle to the simulation data is depicted in Figure 3.

In the main panel, we present the result of an optimized superposition of the $G(t)$ curves at the different temperatures using time shift factors obtained from a least-squares procedure. The latter shift factors are shown in the inset of Figure 3 together with the rheological WLF behavior and the shift factors based on the τ_{av} behavior of $G(t)$. Apparently, the WLF shift factors can provide a satisfactory collapse of the simulated $G(t)$ and incoherent $S(q,t)$ (not shown here) correlation functions onto a single master curve, just like it has been demonstrated for the experimental NSE coherent data.[8] Therefore, the temperature evolution of the segmental relaxation appears to be linked to the τ_{av} behavior related to any correlation function which probes local dynamics.

The main message emerging from the discussion above is that although individual processes (which could selectively be probed by experimental techniques such as in the NMR case) may follow different temperature dependencies (see Figure 2b), it is the behavior of the (process-weighted) average time which leads to an optimized TTS. At this point it must be noticed that as implied from the simulation data, at lower temperatures apart from the t−t and the t−g conformational jumps, additional slower relaxation processes with stronger temperature dependence are expected to contribute to the dynamic spectra.

In the case where only one kind of motion is present, the dynamics detected with different techniques (including NMR) are in reasonable agreement.[13] Thereupon, the additional t−t mechanism existing in PIB modifies the average temperature dependence of the skeletal motion. Moreover, as it is orders of magnitude faster than the t−g transitions, this mechanism essentially provides an additional channel for PIB in order to relax local stresses, resulting into a faster segmental motion (by means of accelerating the average time), i.e., a lower glass transition temperature. The average transition rates of the t−t jumps is higher even than the methyl rotation[17] dynamics. There are clear indications from the analysis of our simulation results (not presented here) that this process facilitates concerted motion of methyl and backbone dynamics through a coupling mechanism, opening a new path for reconciliation of the different interpretations concerning the origin of the β-relaxation in PIB.[23]

To recapitulate, this study illustrates the potential of a detailed and unified approach, based on MD simulations, whereby the elementary motional mechanisms are not only identified and characterized per se, but their impact in experimentally accessible functions is systematically analyzed without any a-priori assumption on dynamical models. For the PIB backbone dynamics, this helped to resolve a controversy on the microscopic interpretation of polymer melt dynamics as probed by different experiments.

Acknowledgment. Financial support from the TMR network "New routes to understanding polymer materials using experiments and realistic modelling", under

Contract ERB-FMRX-CT98-0176, is gratefully acknowledged.

References and Notes

(1) McCrum, N.; Read, B.; Williams, G. *Anelastic and Dielectric Effects in Polymeric Solids;* Wiley: London, 1967.
(2) Boyd, R.; Breitling, S. *Macromolecules* **1972**, *5*, 1.
(3) Suter, U.; Saiz, E.; Flory, P. *Macromolecules* **1983**, *16*, 1317.
(4) Vacatello, M.; Yoon, D. *Macromolecules* **1992**, *25*, 2502.
(5) Cho, D.; Neuburger, N.; Mattice, W. *Macromolecules* **1992**, *25*, 322.
(6) Boyd, R.; Pant, P. *Macromolecules* **1991**, *24*, 6325.
(7) Müller-Plathe, F.; Rogers, S.; van Gusteren, W. *J. Chem. Phys.* **1993**, *98*, 9895.
(8) Richter, D.; Arbe, A.; Colmenero, J.; Monkenbusch, M.; Farago, B.; Faust, R. *Macromolecules* **1998**, *31*, 1133.
(9) Richter, D.; Monkenbusch, M.; Allgeier, J.; Arbe, A.; Colmenero, J.; Farago, B.; Bae, Y.; Faust, R. *J. Chem. Phys.* **1999**, *111*, 6107.
(10) Ferry, J. *Viscoelastic Properties of Polymers;* John Wiley & Sons: New York, 1970.
(11) Ngai, K.; Plazek, D.; Bero, C. *Macromolecules* **1993**, *25*, 4920.
(12) Slichter, W. *J. Polym. Sci., Part C* **1966**, *14*, 133.
(13) Dejean de la Batie, R.; Lauprêtre, F.; Monnerie, L. *Macromolecules* **1989**, *22*, 2617.
(14) Bandis, A.; Wen, W.; Jones, E.; Kaskan, P.; Zhu, Y.; Jones, A.; Inglefield, P.; Bendler, J. *J. Polym. Sci., Polym. Phys. Ed.* **1994**, *32*, 1707.
(15) Törmälä, P. *J. Macromol. Sci., Rev. Macromol. Chem. C* **1979**, *17*, 297.
(16) Forester, T.; Smith, W. CCLRC, Daresbury Laboratory, Daresbury, Warrington Wa4 4AD, England. The MD runs were performed using DL_POLY, the molecular dynamics package developed at Daresbury Laboratory.
(17) Karatasos, K.; Saija, F.; Ryckaert, J.-P. *Physica B* **2001**, *301*, 119.
(18) Arrighi, V.; Higgins, J. *Physica B* **1996**, *226*, 1.
(19) Provencher, S. *Comput. Phys. Commun.* **1982**, *27*, 229.
(20) Moe, N.; Ediger, M. *Macromolecules* **1995**, *28*, 2329.
(21) The static structure as calculated in the present study (not shown here) is in very good agreement with X-ray scattering experiments performed by Londono et al. *J. Polym. Sci., Part B: Polym. Phys.* **1996**, *34*, 3055.
(22) Bée, M. *Quasielastic Neutron Scattering;* Adam Hilger: Bristol, 1988.
(23) Richter, D.; Monkenbusch, M.; Arbe, A.; Colmenero, J.; Farago, B.; Faust, R. *J. Phys.: Condens. Matter* **1999**, *22*, 927.

MA010869H